King Saud University

Journal of King Saud University – Engineering Sciences

www.ksu.edu.sa
www.sciencedirect.com

ORIGINAL ARTICLE

Effect of Hall current and thermal radiation on heat and mass transfer of a chemically reacting MHD flow of a micropolar fluid through a porous medium

J.I. Oahimire [a],*, B.I. Olajuwon [b]

[a] *Department of Mathematics, University of Port Harcourt, Port Harcourt, Nigeria*
[b] *Department of Mathematics, Federal University of Agriculture, Abeokuta, Nigeria*

Abstract   Heat and mass transfer effects on an unsteady flow of a chemically reacting micropolar fluid over an infinite vertical porous plate through a porous medium in the presence of a transverse magnetic field with Hall effect and thermal radiation are studied. The governing system of partial differential equations is transformed to dimensionless equations using dimensionless variables. The dimensionless equations are then solved analytically using the perturbation technique to obtain the expressions for velocity, microrotation, temperature and concentration. With the help of graphs, the effects of the various important parameters entering into the problem on the velocity, microrotation, temperature and concentration fields within the boundary layer are discussed. Also the effects of the pertinent parameters on the skin friction coefficient and rates of heat and mass transfer in terms of the Nusselt number and Sherwood number are presented numerically in a tabular form. The results show that the observed parameters have a significant influence on the flow, heat and mass transfer.

© 2013 Production and hosting by Elsevier B.V. on behalf of King Saud University.

1. Introduction

In many transport processes existing in nature and in industrial applications in which heat and mass transfer is a conse-

* Corresponding author. Tel.: +23408063745591.
  E-mail addresses: imumolen@yahoo.co.uk (J.I. Oahimire), olajuwonishola@yahoo.com (B.I. Olajuwon).
☆ Peer review under responsibility of King Saud University.

Production and hosting by Elsevier

quence of buoyancy effects caused by diffusion of heat and chemical species, the study of such processes is useful for improving a number of chemical technologies such as polymer production, enhanced oil recovery, underground energy transport, manufacturing of ceramics and food processing. Heat and mass transfer from different geometries embedded in porous media has many engineering and geophysical applications such as drying of porous solids, thermal insulations, and cooling of nuclear reactors. At high operating temperature, radiation effects can be quite significant. Many processes in engineering areas occur at high temperature and knowledge of radiation heat transfer becomes very important for the design of reliable equipments, nuclear plants, gas turbines and

various propulsion devices or aircraft, missiles, satellites and space vehicles. Micropolar fluids are those consisting of randomly oriented particles suspended in a viscous medium, which can undergo a rotation that can affect the hydrodynamics of the flow, making it a distinctly non- Newtonian fluid. They constitute an important branch of non-Newtonian fluid dynamics where microrotation effects as well as microinertia are exhibited. The theory of micropolar fluids originally developed by Erigen, 1966 has been a popular field of research in recent years. Eringen's theory has provided a good model for studying a number of complicated fluids, such as colloidal fluids, polymeric fluids and blood. Micropolar fluid flow induced by the simultaneous action of buoyancy forces is of great interest in nature and in many industrial applications as drying processes, solidification of binary alloy as well as in astrophysics, geophysics and oceanography.

When the strength of the magnetic field is strong, one cannot neglect the effect of Hall current. It is of considerable importance and interest to study how the results of the hydrodynamical problems get modified by the effect of Hall currents. Hall currents give rise to a cross flow making the flow three dimensional. Several authors ((Eldabe and ouat, 2006); (Keelson and Desseaux, 2001); (Mahmoud, 2007); (Magdy, 2005); (Modather et al., 2009); (Nadeem et al., 2010); (Omokhuale et al., 2012); (Patil and Kulkarni, 2008); (Rehbi et al., 2007); (Roslinda et al., 2008); (Srinivasachanya and Ramreddy, 2011); (Sunil et al., 2006)) studied MHD flow of a micropolar fluid. Rakesh and Khem (2011) studied the effect of slip conditions and Hall current on unsteady MHD flow of a viscoelastic fluid past an infinite vertical porous plate through a porous medium.

We extended the work of Rakesh and Khem, 2011 by incorporating angular momentum and concentration equations with thermal radiation and chemical reaction terms in the absence of viscoelastic term to study Hall current and thermal radiation on heat and mass transfer of unsteady MHD flow of a chemically reacting micropolar fluid through a porous medium. The governing equations are solved analytically using the perturbation method and the effect of various physical parameters is discussed numerically and graphically.

2. Mathematical Formulation

We consider the unsteady flow of a viscous incompressible and electrically conducting micropolar fluid over an infinite vertical porous plate, subjected to a constant transverse magnetic field B_0 in the presence of thermal and concentration buoyancy effects.
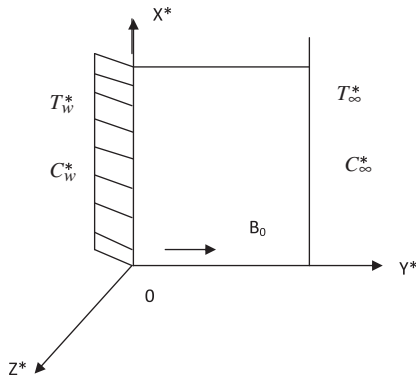

Figure 1 Physical mode.

The induced magnetic field is assumed to be negligible compared to the applied magnetic field. The x^*-axis is taken along the planar surface in the upward direction and the y^*-axis is taken to be normal to it as shown in Fig. 1. Due to the infinite plane surface assumption, the flow variables are functions of y^* and the t^* only. The plate is subjected to a constant suction velocity V_0.

The governing equations of flow under the usual Boussinesq approximation are given by

$$\frac{\partial v^*}{\partial y^*} = 0 \tag{1}$$

$$\frac{\partial u^*}{\partial t^*} + v^* \frac{\partial u^*}{\partial y^*} = (v + v_r)\frac{\partial^2 u^*}{\partial y^{*2}} + v_r \frac{\partial N_1^*}{\partial y^*} + g\beta_T(T^* - T_\infty^*)$$
$$+ g\beta_c(C^* - C_\infty^*) - \sigma\frac{B_0^2(u^* + mw^*)}{\rho(1 + m^2)} - \frac{v}{K^*}u^* \tag{2}$$

$$\frac{\partial w^*}{\partial t^*} + v^* \frac{\partial w^*}{\partial y^*} = (v + v_r)\frac{\partial^2 w^*}{\partial y^{*2}} - v_r \frac{\partial N_2^*}{\partial y^*} - \sigma\frac{B_0^2(w^* - mu^*)}{\rho(1 + m^2)}$$
$$- \frac{v}{K^*}W^* \tag{3}$$

$$\rho J^*\left(\frac{\partial N_1^*}{\partial t^*} + v^*\frac{\partial N_1^*}{\partial y^*}\right) = \gamma\frac{\partial^2 N_1^*}{\partial y^{*2}} \tag{4}$$

$$\rho J^*\left(\frac{\partial N_2^*}{\partial t^*} + v^*\frac{\partial N_2^*}{\partial y^*}\right) = \gamma\frac{\partial^2 N_2^*}{\partial y^{*2}} \tag{5}$$

$$\frac{\partial T^*}{\partial t^*} + v^*\frac{\partial T^*}{\partial y^*} = \frac{k}{\rho C_p}\frac{\partial^2 T^*}{\partial y^{*2}} - \frac{1}{\rho C_p}\frac{\partial q_r}{\partial y^*} \tag{6}$$

$$\frac{\partial C^*}{\partial t^*} + v^*\frac{\partial C^*}{\partial y^*} = D\frac{\partial^2 C^*}{\partial y^{*2}} - K_c^*(C^* - C_\infty^*) \tag{7}$$

The appropriate boundary conditions for the problem are

$$u^* = L^*\left(\frac{\partial u^*}{\partial y^*}\right), v^* = 0, w^* = L^*\left(\frac{\partial u^*}{\partial y^*}\right),$$

$$N_1^* = -n\frac{\partial u^*}{\partial y^*}, N_2^* = n\frac{\partial w^*}{\partial y^*} T^* = T_\infty^* + (T_w^* - T_\infty^*)e^{i\omega^* t^*}$$

$$C^* = C_\infty^* + (C_w^* - C_\infty^*)e^{i\omega^* t^*} \text{ at } y^* = 0$$

$$u^* \to 0, v^* \to 0, w^* \to 0, N_1^* \to 0, N_2^* \to 0 T^* \to T_\infty^*,$$

$$C^* \to C_\infty^* \text{ at } y^* \to \infty \tag{8}$$

where u^*, v^* and w^* are velocity components along x^*, y^* and z^*-axis respectively, N_1^* and N_2^* are microrotation components along x^* and z^*-axis respectively, v is the Kinematic viscosity, v_r is the Kinematic micro-rotation viscosity, q_r is the the radiative heat flux, g is the acceleration due to gravity, βt and βc are the coefficients of thermal expansion and concentration expansion respectively, T^* is the dimensional temperature of the fluid, T_w^* and T_∞^* denote the temperature at the plate and temperature far away from the plate respectively, C^* is the dimensional concentration of the solute, C_w^* and C_∞^* are concentration of the solute at the plate and concentration of the solute far from the plate respectively, K^* is the permeability of the porous medium, k is the thermal conductivity of the medium, ρ is the density of the fluid, j^* is the micro-inertia density or micro-inertia per unit mass, γ is the spin gradient viscosity, L^* is the characteristic length, ω^* is the dimensional frequency of oscillation, σ is the electrical conductivity, m is

the Hall current parameter, K_c^* is the rate of chemical reaction and D is the molecular diffusivity.

The constant that is related to microgyration vector and shear stress is n. Further, $0 \leqslant n \leqslant 1$. The case $n = 0$ represents concentrated particle flows in which the microelement close to the wall surface is unable to rotate. This case is also known as the strong concentration of microelements. The case $n = 0.5$ indicates the vanishing of anti-symmetric part of the stress tensor and denotes weak concentration of microelements. The case $n = 1$ is used for the modeling of turbulent boundary layer flows. We shall consider $n = 0$ and $n = 0.5$.

Following Rosseland approximation, the radiative heat flux q_r is modeled as

$$q_r = \frac{4\sigma^*}{3k^*} \frac{\partial T^{*4}}{\partial y^*} \tag{9}$$

where σ^* is the Stefan–Boltzman constant and k^* is the mean absorption coefficient. Assuming that the difference in temperature within the flow is such that T^{*4} can be expressed as a linear combination of the temperature, we expand T^{*4} in Taylor's series about T_∞^* as follows:

$$T^{*4} = T_\infty^{*4} + 4T_\infty^{*3}(T^* - T_\infty^*) + 6T_\infty^{*2}(T^* - T_\infty^*)^2 + - - - \tag{10}$$

and neglecting higher order terms beyond the first degree in $(T^* - T_\infty^*)$, we have

$$T^{*4} \approx -3T_\infty^{*4} + 4T_\infty^{*3}T^* \tag{11}$$

Differentiating Eq. (9) with respect to y^* and using Eq. (11) to obtain

$$\frac{\partial q_r}{\partial y^*} = \frac{-16T_\infty^3 \sigma^*}{3k*} \frac{\partial^2 T^*}{\partial y^{*2}} \tag{12}$$

Let us introduce the following dimensionless variables:

$$u = \frac{u^*}{V_0}, v = \frac{v^*}{V_0}, W = \frac{w^*}{V_0}\eta = \frac{V_0 y^*}{v}, N_1 = \frac{vN_1^*}{V_0^2}, N_2 = \frac{vN_2^*}{V_0^2} t = \frac{t^* V_0^2}{4v},$$

$$\omega = \frac{4v\omega^*}{V_0^2}, h = \frac{V_0 L^*}{v} \tag{13}$$

$$\theta = \frac{T^* - T_\infty^*}{T_w^* - T_\infty^*}, C = \frac{C^* - C_\infty^*}{C_w^* - C_\infty^*}, J = \frac{V_0^2 J^*}{v^2}$$

Substituting Eq. (13) into Eqs. (2)–(8) and using Eq. (1) yield the following dimensionless equations:

$$\frac{1}{4} \frac{\partial u}{\partial t} - \frac{\partial u}{\partial \eta} = (1+\beta)\frac{\partial^2 u}{\partial \eta^2} + \beta \frac{\partial N_1}{\partial \eta} - \frac{M}{1+m^2}(mw+u) + Gr\theta + GcC - \frac{u}{K} \tag{14}$$

$$\frac{1}{4} \frac{\partial w}{\partial t} - \frac{\partial w}{\partial \eta} = (1+\beta)\frac{\partial^2 w}{\partial \eta^2} - \beta \frac{\partial N_2}{\partial \eta} - \frac{M}{1+m^2}(w-mu) - \frac{u}{K} \tag{15}$$

$$\frac{1}{4} \frac{\partial N_1}{\partial t} - \frac{\partial N_1}{\partial \eta} = L\frac{\partial^2 N_1}{\partial \eta^2} \tag{16}$$

$$\frac{1}{4} \frac{\partial N_2}{\partial t} - \frac{\partial N_2}{\partial \eta} = L\frac{\partial^2 N_2}{\partial \eta^2} \tag{17}$$

$$\frac{1}{4} \frac{\partial \theta}{\partial t} - \frac{\partial \theta}{\partial \eta} = \frac{1}{Pr}(1+Nr)\frac{\partial^2 \theta}{\partial \eta^2} \tag{18}$$

$$\frac{1}{4} \frac{\partial C}{\partial t} - \frac{\partial C}{\partial \eta} = \frac{1}{Sc} \frac{\partial^2 C}{\partial \eta^2} - K_c C \tag{19}$$

where $\beta = \frac{v_r}{v}$ is the dimensionless viscosity ratio, $Nr = \frac{16T_\infty^* \sigma^*}{3k^* k}$ is the thermal radiation parameter, $M = \frac{\sigma B_0^2 v}{\rho V_0^2}$ is the magnetic field parameter, $Gr = \frac{v\beta_t g(T_w^* - T_\infty^*)}{V_0^3}$ is the Grashof number, $Gc = \frac{v\beta_c g(C_w^* - C_\infty^*)}{V_0^3}$ is the modified Grashof number, $Pr = \frac{v\rho C_p}{K}$ is the Prandtl number, $Sc = \frac{v}{D}$ is the Schmidt number, $K = \frac{K^* V_0^2}{v^2}$ is the permeability of the porous medium parameter and $L = \frac{\gamma V_0^2}{\rho v^3 j}$ is the material parameter and K_c is the chemical reaction parameter.

Also the boundary conditions become

$$u = h\frac{\partial u}{\partial \eta}, v = 0, w = h\frac{\partial w}{\partial \eta}, \theta = e^{i\omega t}, C = e^{i\omega t}, N_1 = -n\frac{\partial u}{\partial \eta}, N_2 = n\frac{\partial w}{\partial \eta} \text{ at } y = 0$$
$$u \to 0, v \to 0, w \to 0, \theta \to 0, C \to 0, N_1 \to 0, N_2 \to 0 \text{ at } y \to \infty \tag{20}$$

where $h = \frac{V_0 L^*}{v}$ is the slip parameter.

We now simplified (14)–(17) by introducing $q = u + iw$ and $p = N_1 + iN_2$ to have

$$\frac{1}{4} \frac{\partial q}{\partial t} - \frac{\partial q}{\partial \eta} = (1+\beta)\frac{\partial^2 q}{\partial \eta^2} + i\beta \frac{\partial p}{\partial \eta} - \frac{M}{1+m^2}(1-im)q + Gr\theta + GcC - \frac{q}{K} \tag{21}$$

$$\frac{1}{4} \frac{\partial p}{\partial t} - \frac{\partial p}{\partial \eta} = L\frac{\partial^2 p}{\partial \eta^2} \tag{22}$$

$$\frac{1}{4} \frac{\partial \theta}{\partial t} - \frac{\partial \theta}{\partial \eta} = \frac{1}{Pr}(1+Nr)\frac{\partial^2 \theta}{\partial \eta^2} \tag{23}$$

$$\frac{1}{4} \frac{\partial C}{\partial t} - \frac{\partial C}{\partial \eta} = \frac{1}{Sc} \frac{\partial^2 C}{\partial \eta^2} - K_c C \tag{24}$$

And the corresponding boundary conditions are

$$q = h\frac{\partial q}{\partial \eta}, \theta = e^{i\omega t}, C = e^{i\omega t}, P = \text{in}\frac{\partial q}{\partial \eta}, \text{ at } y = 0$$
$$q \to 0, \theta \to 0, C \to 0, P \to 0, \text{ at } y \to \infty \tag{25}$$

5. Method of Solution

In order to solve Eqs. (21)–(24) subject to the boundary conditions (25), we assume a perturbation of the form:

$$q = q_0(\eta)e^{i\omega t}, P = P_0(\eta)e^{i\omega t}, \theta_0(\eta)e^{i\omega t}, C = C_0(\eta)e^{i\omega t} \tag{26}$$

Substituting Eq. (26) into Eqs. (21)–(24), we obtain the following set of equations:

$$a_1 q_0'' + q_0' - a_2 q_0 = -Gr\theta_0 - GcC_0 - i\beta P_0' \tag{27}$$

$$LP_0'' + P_0' - \frac{i\omega}{4} P_0 = 0 \tag{28}$$

$$a_3 \theta_0'' + \theta_0' - \frac{i\omega}{4} \theta_0 = 0 \tag{29}$$

$$C_0'' + ScC_0' - a_4 C_0 = 0 \tag{30}$$

where $a_1 = 1+\beta, a_2 = i\left(\frac{w}{4} - \frac{Mm}{1+m^2}\right) + \frac{M}{1+m^2} + \frac{1}{K}, a_3 = \frac{1+Nr}{Pr}, a_4 = \left(\frac{i\omega}{4} + Kc\right)$

The corresponding boundary conditions can be written as

$$q_0 = h\frac{\partial q_0}{\partial \eta}, \theta_0 = 1, C_0 = 1, P_0 = in\frac{\partial q_0}{\partial \eta}, \text{ at } y = 0$$
$$q_0 = 0, \theta_0 = 0, C_0 = 0, P_0 = 0, \text{ at } y \to \infty \tag{31}$$

Table 1 Effect of n, Nr, m and Kc parameter on C_f and $C'w$ with $K = 1$, $t = 1$, $\omega = 0.01$, $\beta = 0.5$, $Gr = 1$, $Gc = 1$, $M = 2$, $Pr = 1$, $L = 1$, $Sc = 1$, $h = 0.1$.

N	Nr	m	Kc	C_f	$C'w$
0	0.5	0.2	0.1	1.0014	0
0.5	0.5	0.2	0.1	0.3346	0.0198
1	0.5	0.2	0.1	-0.0601	0.0215
0.5	0.2	0.2	0.1	0.2763	0.0148
0.5	0.4	0.2	0.1	0.3181	0.0184
0.5	0.8	0.2	0.1	0.3734	0.0231
0.5	0.5	0.3	0.1	0.3405	0.0285
0.5	0.5	0.4	0.1	0.3483	0.0365
0.5	0.5	0.5	0.1	0.3577	0.0437
0.5	0.5	0.2	0.2	0.2945	0.0172
0.5	0.5	0.2	0.3	0.2523	0.0138
0.5	0.5	0.2	0.4	0.2063	0.0095

The solution of (27)–(30) satisfying the boundary conditions (31) is given by

$$q = (A_1 e^{-r_4\eta} + A_2 e^{-r_2\eta} + A_3 e^{-r_3\eta} + A_4 e^{-r_1\eta})e^{i\omega t} \quad (32)$$

$$P = B_1 e^{i\omega t - r_1\eta} \quad (33)$$

$$\theta = e^{i\omega t - r_2\eta} \quad (34)$$

$$C = e^{i\omega t - r_3\eta} \quad (35)$$

where

$$a_1 = 1 + \beta$$

$$a_2 = i\left(\frac{w}{4} - \frac{Mm}{1+m^2}\right) + \frac{M}{1+m^2} + \frac{1}{K}$$

$$a_3 = \frac{1 + Nr}{Pr}$$

$$a_4 = \left(\frac{i\omega}{4} + Kc\right)$$

$$r_1 = \frac{1 + \sqrt{1 + i\omega L}}{2L}$$

$$r_2 = \frac{1 + \sqrt{1 + i\omega a_3}}{2a_3}$$

$$r_3 = \frac{Sc + \sqrt{Sc^2 + 4a_4}}{2}$$

$$r_4 = \frac{1 + \sqrt{1 + 4a_1 a_2}}{2a_1}$$

$$A_2 = \frac{-Gr}{r_2^2 a_1 - r_2 - a_2}$$

$$A_3 = \frac{-Gc}{r_3^2 a_1 - r_3 - a_2}$$

$$A_4 = \frac{-r_1\beta nr_4(hr_2 A_2 + hr_3 A_3 + A_2 + A_3) + (1 + hr_4)\beta r_1 n(r_2 A_2 + r_3 A_3)]}{(r_1^2 a_1 - r_1 - a_2 - \beta r_1^2 n)(1 + hr_4) + \beta r_1 nr_4(hr_1 + 1)}$$

$$A_1 = \frac{-h(r_2 A_2 + r_3 A_3 + r_1 A_4) - (A_2 + A_3 + A_4)}{(1 + hr_4)}$$

Table 2 Effect of Pr and Nr parameter on $NuRe_x^{-1}$ with $n = 0.5$, $K = 1$, $\beta = 0.5$, $Gr = 1$, $Gc = 1$, $M = 2$, $Pr = 1$, $\omega = 0.01$, $t = 1$, $L = 1$, $m = 0.2$, $h = 0.2$, $Kc = 0.1$.

Pr	Nr	$NuRe_x^{-1}$
0.8	0.5	0.5333
1.2	0.5	0.7999
1.4	0.5	0.9333
1	0.2	0.8333
1	0.4	0.7142
1	0.8	0.5555

Table 3 Effect of Sc and Kc parameter on $ShRe_x^{-1}$ with $n = 0.5$, $m = 0.2$, $h = 0.2$, $\beta = 0.5$, $Gr = 2$, $Gc = 1$, $M = 2$, $Pr = 1$, $K = 1$, $L = 1$, $Nr = 0.5$, $\omega = 0.01$, $t = 1$.

Sc	Kc	$ShRe_x^{-1}$
2	0.1	2.0953
3	0.1	3.0967
4	0.1	4.0974
1	0.2	1.1707
1	0.3	1.2415
1	0.4	1.3061

$$B_1 = -ni(r_4 A_1 + r_2 A_2 + r_3 A_3 + r_1 A_4)$$

The results are presented as velocity, microrotation, temperature and concentration profiles in Figs. 2–23 below;

The local skin friction coefficient, couple stress coefficient, Nusselt number and Sherwood number are important physical quantities of engineering interest. The skin friction coefficient (Cf) at the wall is given by

$$Cf = \frac{\tau_w}{\rho V_0^2} = [1 + (1-n)L]q'(0)$$
$$= -[1 + (1-n)L][r_4 A_1 + r_2 A_2 + r_3 A_3 + r_1 A_4]e^{i\omega t} \quad (36)$$

where τ_w^* is the skin friction

The couple stress coefficient (C'_w) at the plate is written as

$$C'_w = \frac{M_w v^2}{\gamma V_0^3} = p'(0) = -r_1 B_1 e^{i\omega t} \quad (37)$$

where M_w is the wall couple stress.

The rate of heat transfer at the surface in terms of the Nusselt number is given by

$$Nu = \frac{x\left(\frac{\partial T}{\partial y^*}\right)}{(T_\infty^* - T_w^*)}$$

$$NuRe_x^{-1} = -\theta'(0) = r_2 e^{i\omega t} \tag{38}$$

where $Re_x = \frac{xV_0}{v}$

The rate of mass transfer at the surface in terms of the local Sherwood number is given by

$$Sh = \frac{\left(\frac{\partial C^*}{\partial y^*}\right)_{y^*=0}}{C_\infty^* - C_w^*}$$

$$ShRe_x^{-1} = -C'(0) = r_3 e^{i\omega t} \tag{39}$$

The numerical results for skin friction coefficient, couple stress coefficient, Nusselt number and Sherwood number are shown in Tables 1–3 below:

6. Discussion

Unsteady incompressible and electrically three-dimensional flow of a chemically reacting micropolar fluid over an infinite vertical porous plate through a porous medium was studied. Numerical evaluation of the analytical solutions reported in the previous section was performed and the results are presented in graphical and tabular forms. This was done to illustrate the influence of various parameters involved. In this study, we have chosen $t = 1$ and $\omega = 0.01$ while other parameters are varied over a range.

The effect of magnetic field parameter on velocity distribution profiles across the boundary layer is presented in Fig. 2. It is obvious that the effect of increasing values of the magnetic field parameter M results in a decreasing velocity distribution across the boundary layer. This is due to the fact that the effect of a transverse magnetic field gives rise to a resistive type-force called the Lorentz force. The force has the tendency to slow the
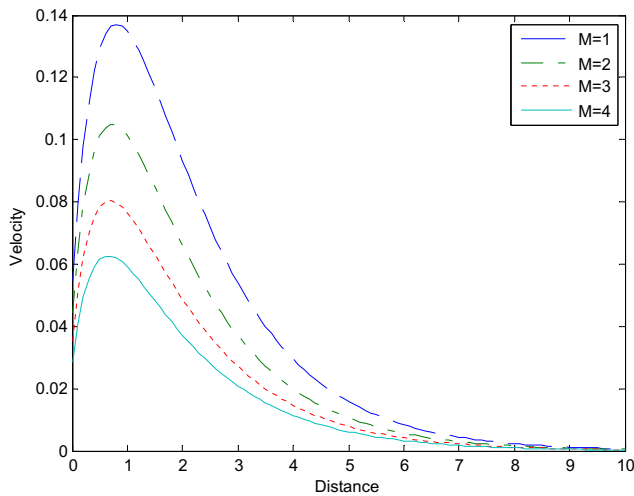
Figure 2 Velocity profiles with different values of magnetic parameter.
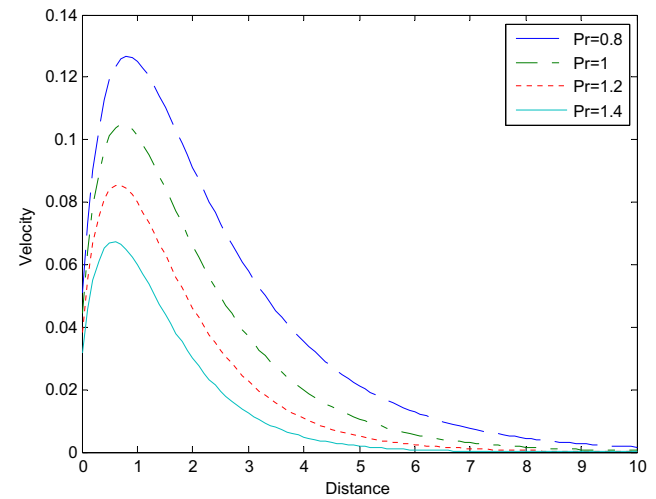
Figure 4 Velocity profiles with different values of the Prandtl number.
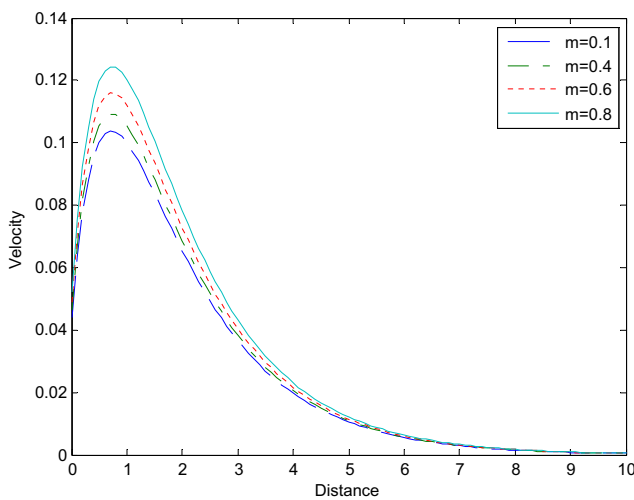
Figure 3 Velocity profiles with different values of Hall current parameter.
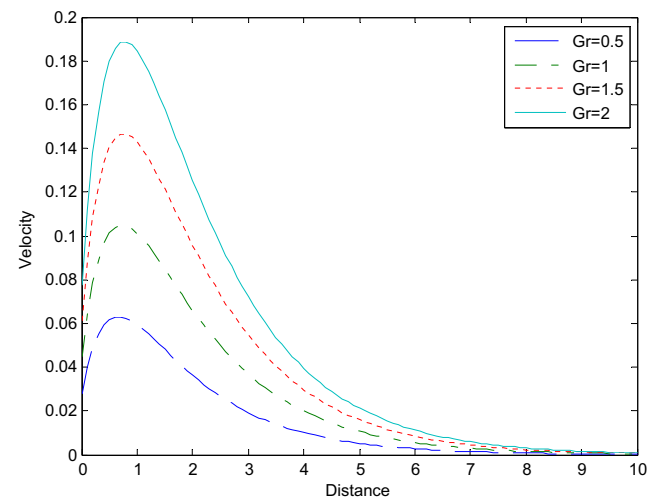

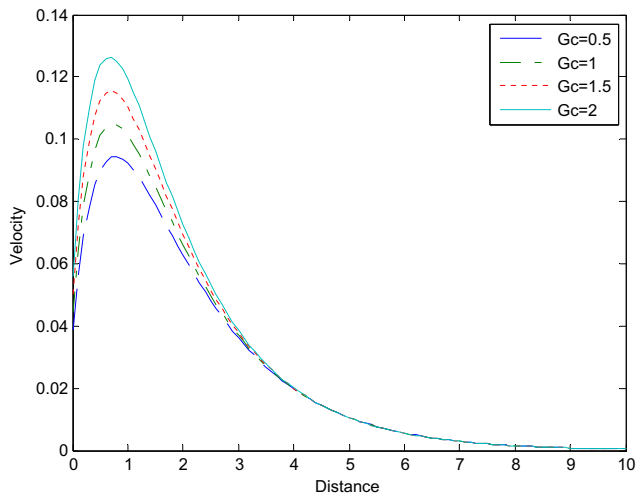**Figure 5** Velocity profiles with different values of the Grashof number.

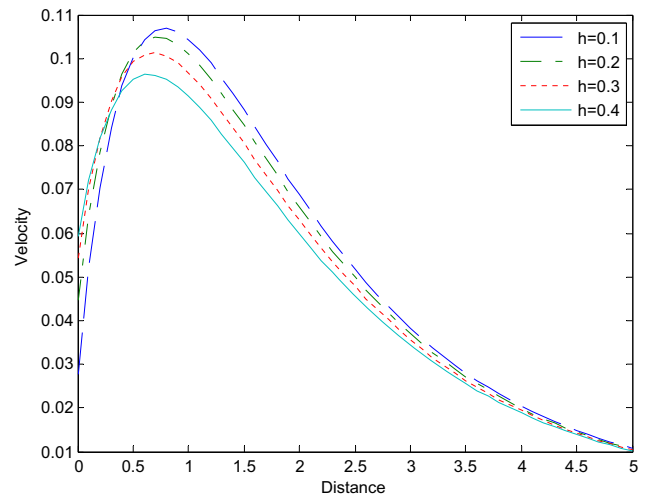**Figure 6** Velocity profiles with different values of the modified Grashof number.

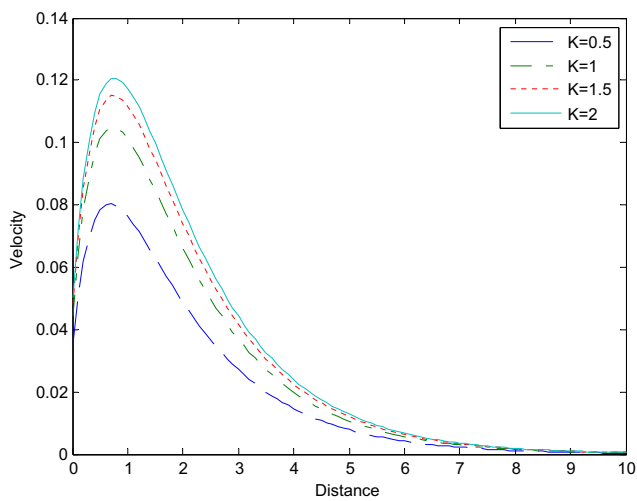**Figure 9** Velocity profiles with different values of slip parameter.

Figure 7 Velocity profiles with different values of permeability of the porous medium parameter.
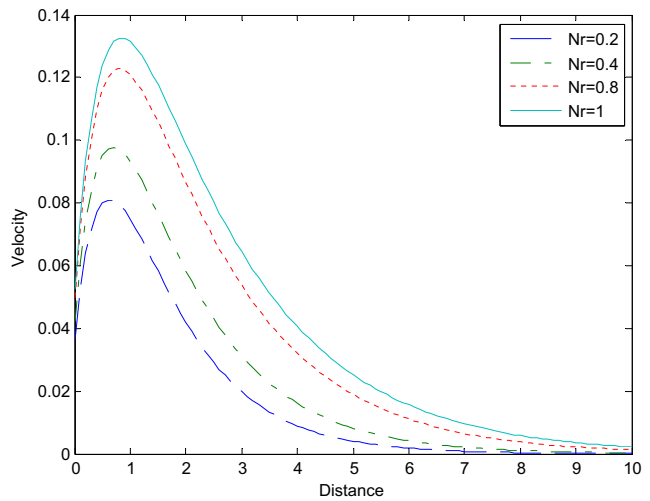

Figure 10 Velocity profiles with different values of radiation parameter.
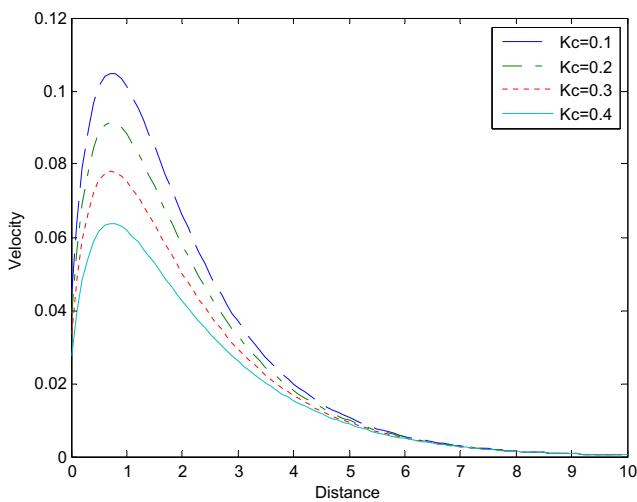

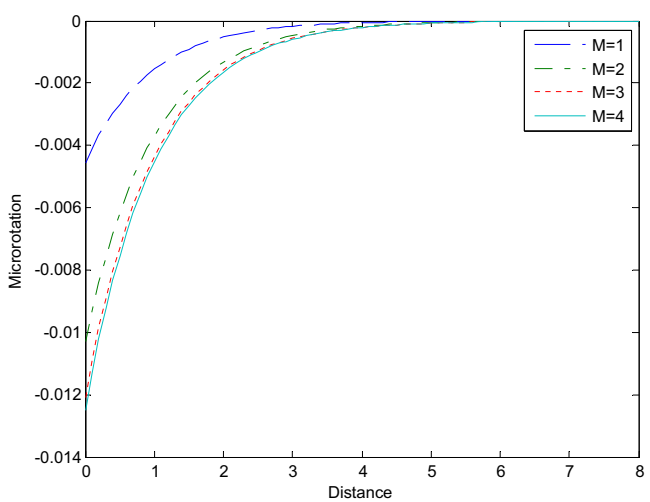**Figure 8** Velocity profiles with different values of chemical reaction parameter.

Figure 11a Microrotation profiles with different values of magnetic field parameter when $n = 0.5$.
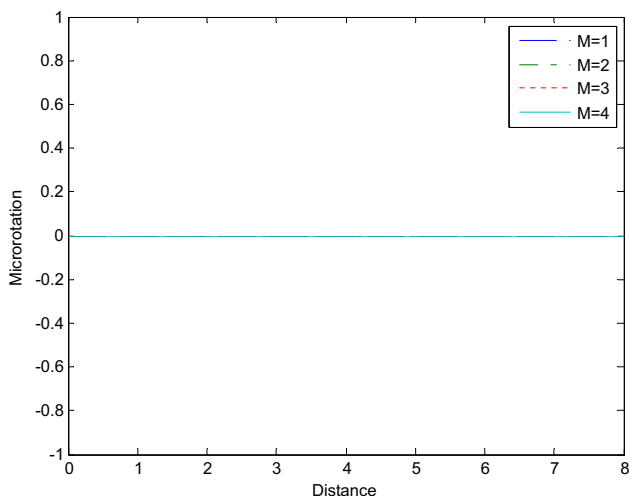
Figure 11b Microrotation profiles with different values of magnetic field parameter when $n = 0$.
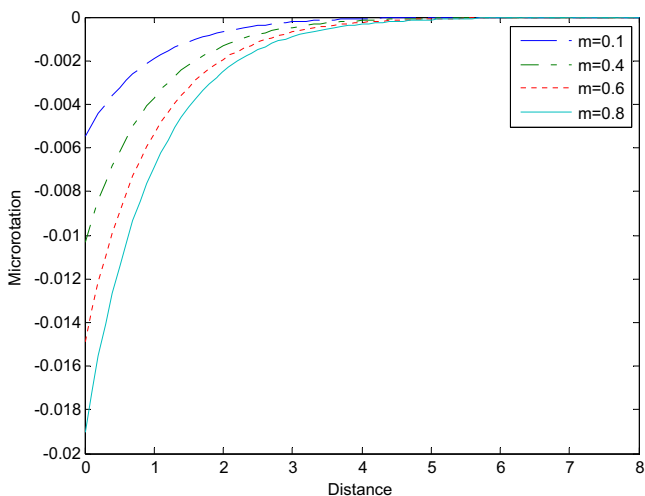

Figure 12 Microrotation profiles with different values of Hall current parameter.

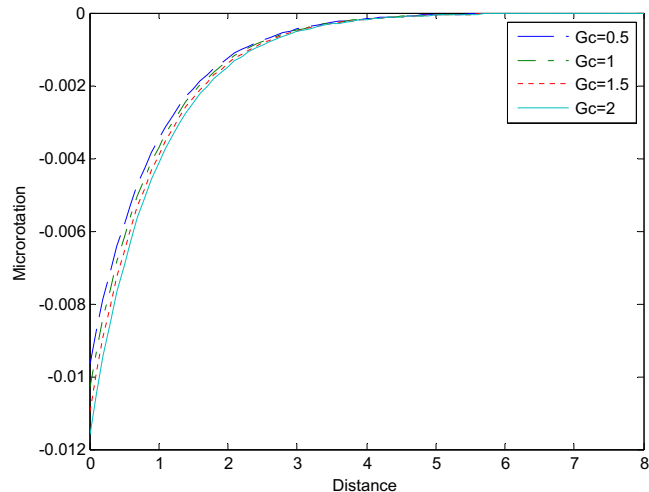**Figure 13** Microrotation profiles with different values of the Prandtl number.

Figure 14 Microrotation profiles with different values of the Grashof number.
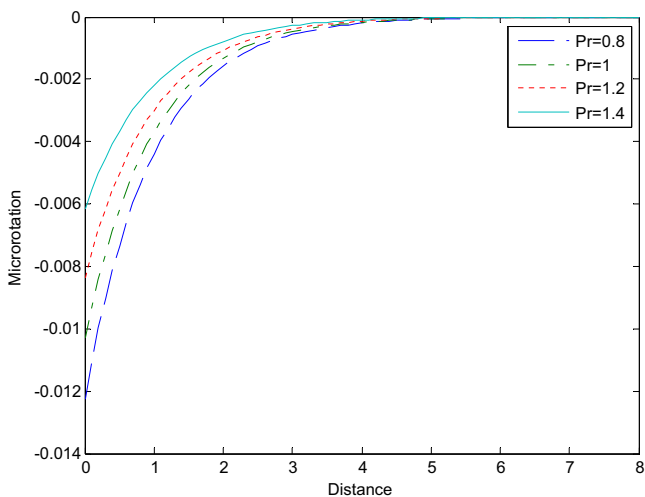

Figure 15 Microrotation profiles with different values of the modified Grashof number.

motion of the fluid. Fig. 3 displays the effect of Hall current parameter on the translational velocity distribution profiles. It is noticed that the Hall current parameter increases the velocity. Fig. 4 presents the translational velocity distribution profiles for different values of the Prandtl number (Pr). The results show that the effect of increasing values of the prandtl number results in a decrease in the velocity. Figs. 5 and 6 illustrate the translational velocity profiles for different values of the Grashof number (Gr) and modified Grashof number (Gc) respectively. It can be seen that an increase in Gr or Gc leads to a rise in velocity profiles. Fig. 7 depicts the effect of permeability of the porous medium parameter (K) on translational velocity distribution profiles and it is obvious that as permeability parameter (K) increases, the velocity increases along the boundary layer thickness which is expected since when the holes of porous medium become larger, the resistive of the medium may be neglected. Fig. 8 shows the influence of the chemical reaction parameter on translational velocity

profiles. The velocity decreases as the parameter increases. Fig. 9 illustrates the variation of slip parameter with translational distribution profiles. It can be observed from the figure that the velocity increases with increasing value of the parameter near the plate and starts decreasing away from the plate. Fig. 10 shows the translational velocity profiles with different values of radiation parameter. And the effect of increasing the radiation parameter is to increase the translational velocity. This is because when the intensity of heat generated through thermal radiation is increased, the bond holding the components of the fluid particles is easily broken and the fluid velocity is increased.

Figs. 11a and b depict the microrotational velocity profiles for different values of magnetic field parameter respectively. The microrotational velocity distribution profiles decrease with an increase in the magnetic field parameter when $n = 0.5$ while it remains constant when $n = 0$ as shown in Fig. 11b. It is clear

from these figures that microrotational effect is more pronounced for $n = 0.5$ in comparison to when $n = 0$. Fig. 12 illustrates the microrotational velocity distribution for different values of Hall current parameter. The figure shows that as Hall current parameter increases, microrotational velocity decreases. Fig. 13 shows that as the Prandtl number increases, microrotational velocity increases. Figs. 14 and 15 elucidate that the effect of increasing Gr or Gc is to decrease microrotational velocity. The effects due to permeability of the porous medium parameter (K) on microrotational velocity are shown in Fig. 16. It is observed that as the parameter increases, the microrotational velocity decreases. Fig. 17 illustrates the microrotational velocity distribution for different values of chemical reaction parameter. The figure shows that as chemical reaction parameter increases, the microrotational velocity increases. Fig. 18 shows that the effect of increasing slip parameter is to increase the microrotational velocity. Fig. 19
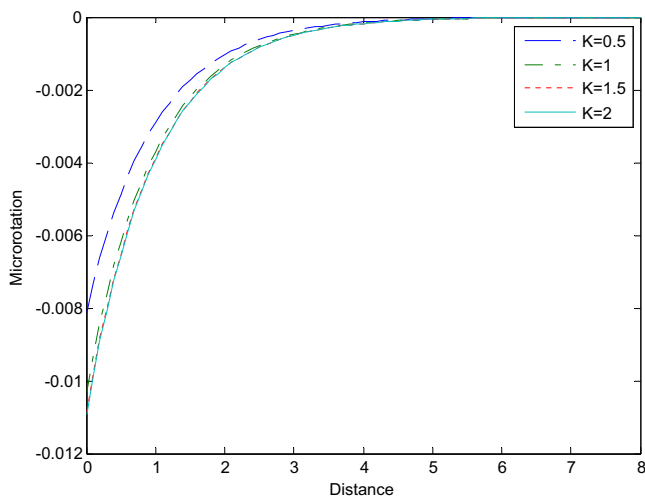

Figure 16 Microrotation profiles with different values permeability of porous medium parameter.
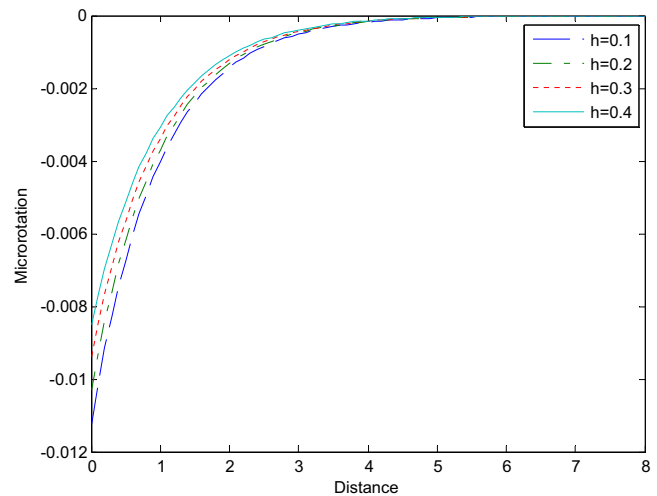

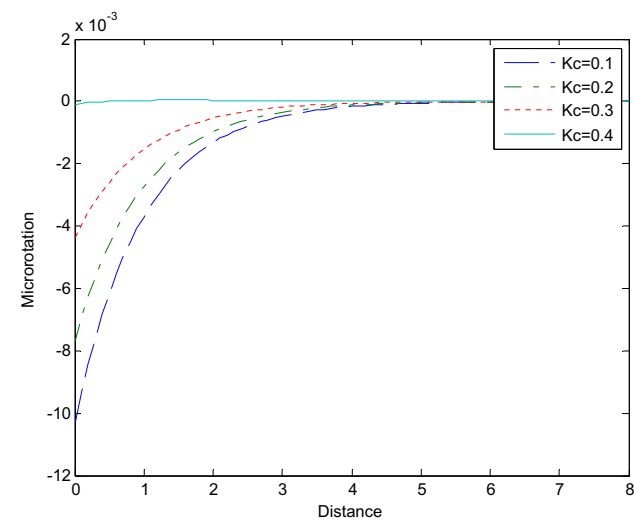**Figure 18** Microrotation profiles with different values of slip parameter.

Figure 17 Microrotation profiles with different values of chemical reaction parameter.
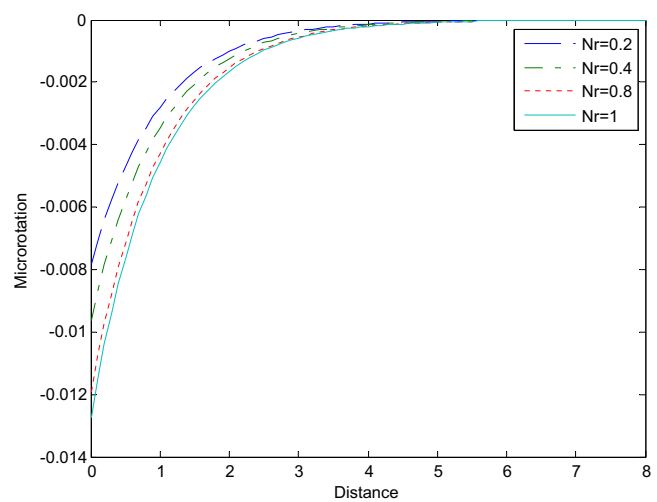

Figure 19 Microrotation profiles with different values of radiation parameter.

illustrates the effect of radiation parameter on microrotational velocity profiles. The profiles decrease as the parameter increases. The microrotation profiles are negative because the microrotation of the fluid is anti-clockwise. Fig. 20 presents the effect of the Prandtl number Pr on the temperature profiles. Increasing the value of Pr has the tendency to decrease the fluid temperature in the boundary layer as well as the thermal boundary layer thickness. This causes the wall slope of the temperature to decrease as Pr is increasing causing the Nusselt number to increase as can be clearly seen in Table 2. Fig. 21 shows the influence of radiation parameter on temperature profiles. It is observed that as radiation parameter increases, the temperature of the fluid increases. Figs. 21 and 22 show concentration distribution profiles for different values of Sc and Kc. It can be noted from these figures that the concentration of the fluid decreases as the parameters increase.

Table 1 shows the effects of constant that is related to microgyration vector and shear stress (n), chemical reaction parameter (Kc), Hall current parameter (m) and radiation parameter (Nr) on skin friction coefficient and couple stress coefficient. It is observed that an increase in the value of n decreases skin friction coefficient which is not surprising since $n = 0$ represents strong concentration and $n = 0.5$ represents weak concentration of the microelements while couple stress coefficient increases with an increase in n. An increase in radiation parameter (Nr) and Hall current parameter (m) increases both skin friction coefficient and couple stress coefficient while an increase in chemical reaction parameter (Kc) decreases them. Table 2 shows the effect of the Prandtl number (Pr) and radiation parameter (Nr) on the Nusselt number. The Nusselt number increases as the Pr number increases and decreases as the radiation parameter increases. This shows that the surface heat transfer from the porous plate increases with the increasing values of Pr and decreases with increasing values of Nr. Table 3 shows that the effect of increasing the Sc and Kc is to increase the rate of mass transfer. These results are in good agreement with Mahmoud, 2007 and Rakesh and Khem, 2011.
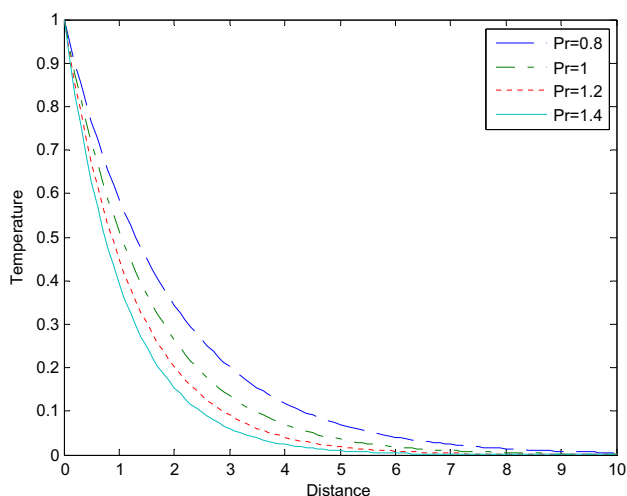

Figure 20 Temperature profiles with different values of the Prandtl number.
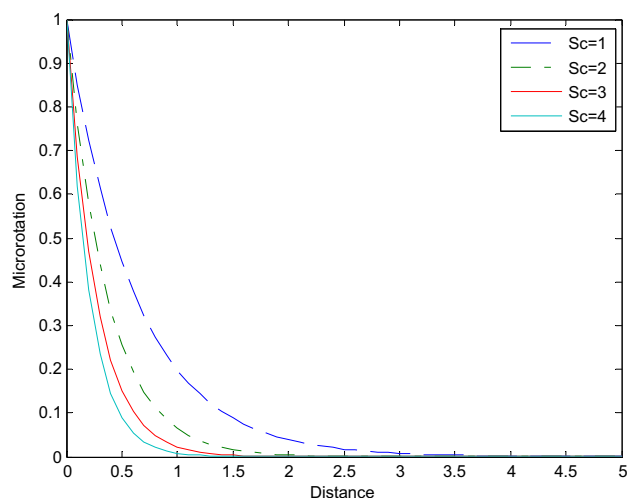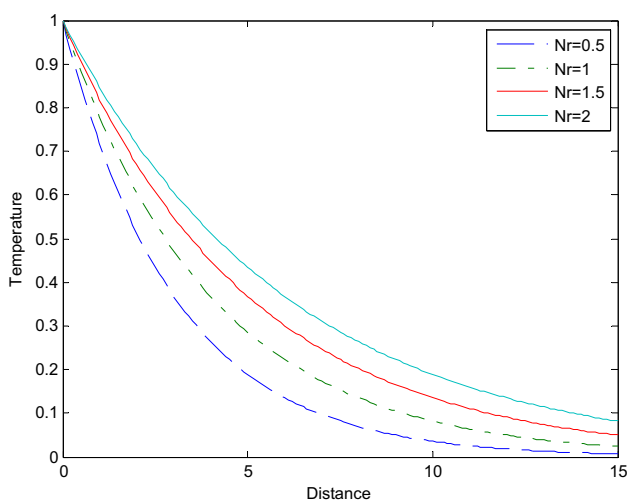

Figure 21 Temperature profiles with different values of radiation parameter.

Figure 22 Concentration profiles with different values of the Schmidt number.
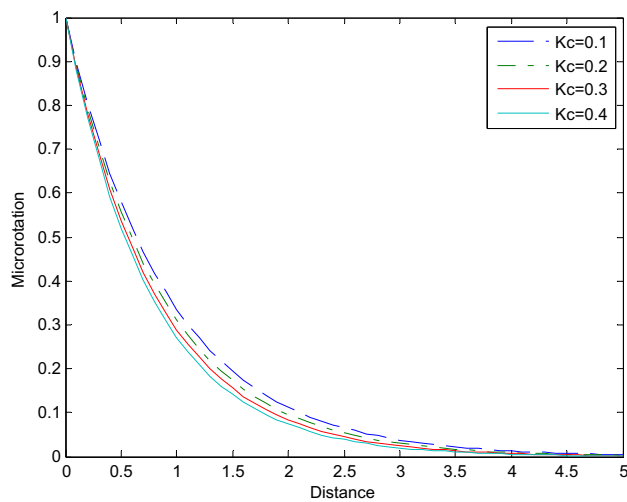

Figure 23 Concentration profiles with different values of chemical reaction parameter.

7. Conclusion

An analytical study of the MHD heat and mass transfer flow of an incompressible, electrically conducting micropolar fluid with chemical reaction over an infinite vertical porous plate through porous medium was conducted. The results are discussed through graphs and tables for different values of parameters entering into the problem. Following conclusions can be drawn from the results obtained:

* In the presence of a uniform magnetic field, increases in the strength of the applied magnetic field decelerated the fluid motion along the wall of the plate inside the boundary layer.
* An increase in Hall current and radiation parameter increases the momentum and thermal boundary layer thickness while they decelerate microrotational velocity.
* The Nusselt number increased as the Prandtl number increased and decreased as radiation parameter increased.
* The Sherwood number increased as the Schmidt number and chemical reaction parameter increased.
* The chemical reaction parameter increases both skin friction coefficient and couple stress coefficient.

Acknowledgement

References

Erigen, A.C., 1966. Theory of micropolar fluids. J. Math. Mech. 16, 1–18.

Eldabe, N.T., Ouat, M.E., 2006. Chebyshew finite difference method for heat and mass transfer in hydromagnetic flow of a micropolar fluid past a stretching surface with Ohmic heating and viscous dissipation. Appl. Math. Comput. 177, 561–571.

Keelson, N.A., Desseaux, A., 2001. Effects of surface condition on flow of a micropolar fluid driven by a porous stretching sheet. Int. J. Eng. Sci. 39, 1881–1897.

Mahmoud, M.A.A., 2007. Thermal radiation effects on MHD flow of a micropolar fluid over a stretching surface with variable thermal conductivity. Physical A 375, 401–410.

Magdy, A.C., 2005. Free convection flow of conducting micropolar fluid with thermal relaxation including heat sources. J. Appl. Math. 2, 271–292, 70.4.

Modather, M., Rashad, A.M., Chamkha, A.J., 2009. Study of MHD heat and mass transfer oscillatory flow of a micropolar fluid over a vertical permeable plate in a porous medium. Turkis J. Eng. Env. Sci. 33, 245–257.

Nadeem, S., Hussain, M., Naz, M., 2010. MHD stagnation flow of a micropolar fluid through a porous medium. Int. J. Meccanica 45, 869–880.

Omokhuale, E., Uwanta, I.J., Momoh, A.A., 2012. The effect of concentration and Hall current on unsteady flow of a viscoelastic fluid in a fixed plate. Int. J. Eng. Res. Appl. 2, 885–892.

Patil, P.M., Kulkarni, P.S., 2008. Effects of chemical reaction on free convective flow of a polar fluid through a porous medium in the presence of internal heat generation. Int. Therm. Sci. 4, 1043–1054.

Rehbi, A.D., Tariq, A.A., Benbella, A.S., Mahoud, A.A., 2007. Unsteady natural convection heat transfer of micropolar fluid over a vertical surface with constant heat flux. Turkish J. Eng. Env. Sci. 31, 225–233.

Roslinda, N., Anuar, I., Ioan, P., 2008. Unsteady boundary layer flow over a stretching sheet in a micropolar fluid. Int. J. Eng. Appl. Sci. 4, 7.

Rakesh, K., Khem, C., 2011. Effect of slip conditions and Hall current on unsteady MHD flow of a viscoelastic fluid past an infinite vertical porous plate through porous medium. Int. J. Eng. Sci. Technol. 3 (4), 0975–5462.

Srinivasachanya, D., Ramreddy, C.H., 2011. Soret and Dufour effect on mixed convection in a non-Darcy porous medium saturated with micropolar fluid. Non Anal. Model. Control 16 (1), 100–115.

Sunil, A., Sharma, A., Bharti, P.K., Shandi, R.G., 2006. Effect of rotation on a layer of micropolar ferromagnetic fluid heated from below saturating a porous medium. Int. J. Eng. Sci. 44 (11–12), 683–698.